In Vivo Transcriptional Activation Using CRISPR/Cas9 in *Drosophila*

Shuailiang Lin,[*,†,1] **Ben Ewen-Campen,**[†,1,2] **Xiaochun Ni,**[†] **Benjamin E. Housden,**[†] **and Norbert Perrimon**[†,2,‡]

*Tsinghua-Peking–National Institute of Biological Sciences Center for Life Sciences, School of Life Sciences, Tsinghua University, Beijing 100084, China, and [†]Department of Genetics, and [‡]Howard Hughes Medical Institute, Harvard Medical School, Boston, Massachusetts 02115

ABSTRACT A number of approaches for Cas9-mediated transcriptional activation have recently been developed, allowing target genes to be overexpressed from their endogenous genomic loci. However, these approaches have thus far been limited to cell culture, and this technique has not been demonstrated *in vivo* in any animal. The technique involving the fewest separate components, and therefore the most amenable to *in vivo* applications, is the dCas9-VPR system, where a nuclease-dead Cas9 is fused to a highly active chimeric activator domain. In this study, we characterize the dCas9-VPR system in *Drosophila* cells and *in vivo*. We show that this system can be used in cell culture to upregulate a range of target genes, singly and in multiplex, and that a single guide RNA upstream of the transcription start site can activate high levels of target transcription. We observe marked heterogeneity in guide RNA efficacy for any given gene, and we confirm that transcription is inhibited by guide RNAs binding downstream of the transcription start site. To demonstrate one application of this technique in cells, we used dCas9-VPR to identify target genes for Twist and Snail, two highly conserved transcription factors that cooperate during *Drosophila* mesoderm development. In addition, we simultaneously activated both Twist and Snail to identify synergistic responses to this physiologically relevant combination. Finally, we show that dCas9-VPR can activate target genes and cause dominant phenotypes *in vivo*, providing the first demonstration of dCas9 activation in a multicellular animal. Transcriptional activation using dCas9-VPR thus offers a simple and broadly applicable technique for a variety of overexpression studies.

KEYWORDS CRISPR-Cas9; gene activation; overexpression, gain-of-function

I T has recently become possible to activate transcription of target genes from their native genomic locus using nuclease-dead Cas9 (dCas9) fused to transcriptional activator domains (Mali *et al.* 2013; Gilbert *et al.* 2014; Tanenbaum *et al.* 2014; Zalatan *et al.* 2014; Chavez *et al.* 2015; Konermann *et al.* 2015). Activating genes from their endogenous transcription start site (TSS) offers several benefits that are complementary to traditional overexpression studies based on cloned cDNAs. For example, the dCas9-mediation activation technique is preferable for genes that are difficult to clone, *e.g.*, if they occur in multiple splice isoforms and/or are very large. In addition, there is evidence that dCas9-mediated activation leads to target gene activation at physiologically relevant levels,

as opposed to many existing techniques (Chavez *et al.* 2015). Cas9-mediated activation also has the benefits that it is easily multiplexed and that it is rapidly scalable for genome-wide studies because the target specificity is provided by easy-to-synthesize 20-bp single guide RNAs (sgRNAs) (Gilbert *et al.* 2014; Chen *et al.* 2015; Konermann *et al.* 2015).

The first attempts to activate transcription by fusing dCas9 to activator domains such as VP64 yielded very low levels of overexpression (Gilbert *et al.* 2013; Maeder *et al.* 2013; Mali *et al.* 2013; Perez-Pinera *et al.* 2013). However, three strategies to substantially increase the effectiveness of dCas9 activators have subsequently been described. In the dCas9-VPR system (Chavez *et al.* 2015), dCas9 is directly fused to a chimeric activator (composed of the **V**P64, **p**65, and **R**ta domains), based on a systematic screen of 20 candidate activator domains. In a second strategy, termed "SunTag" (Gilbert *et al.* 2014; Tanenbaum *et al.* 2014), dCas9 is fused to multiple copies of an epitope tag and is cotransfected with a single-chain antibody fused to the VP64 activator domain, thus recruiting multiple VP64 domains to each molecule of dCas9. The third strategy, which has been developed independently by two groups (Zalatan *et al.* 2014; Konermann

et al. 2015), involves inserting specific RNA hairpin sequences into exposed portions of the sgRNA, and co-expressing proteins that specifically recognize these hairpin sequences and are fused to additional activator domains.

While all of these approaches show promise in cell culture, none has yet been demonstrated *in vivo* in any multicellular animal. We reasoned that, because the dCas9-VPR system requires a single activator component in addition to the sgRNA, it would be most amenable to stable transgenesis for *in vivo* studies. dCas9-VPR has been shown to efficiently activate gene expression in yeast, human, mouse, and *Drosophila* cells, yet previous studies in *Drosophila* cells have been limited to just two target genes and utilized pools of up to five sgRNAs per gene (Chavez *et al.* 2015). In this study, we first show that dCas9-VPR functions robustly in *Drosophila* cells on an array of target genes, both singly and in multiplex. We test a number of sgRNAs per target gene and conclude that a single highly active sgRNA is sufficient to activate transcription and that there is substantial variability in sgRNA effectiveness. We also confirm previous observations that target gene activation levels are inversely proportional to their basal expression levels. We use dCas9-VPR to activate the transcription factors Twist and Snail in cells, both singly and together, and then use RNAseq to identify transcriptional targets of these two conserved factors. Finally, we adapt the dCas9-VPR system for Gal4-UAS activation and show that this approach can activate target genes *in vivo* at levels sufficient to induce dominant phenotypes. Together, our results demonstrate the ease and utility of the dCas9-VPR system in *Drosophila* cells and *in vivo*.

Materials and Methods

Cloning of Cas9 activators and sgRNA

dCas9-VPR has been previously described (Chavez *et al.* 2015). UAS-driven transgenes were cloned into pWalium20 (Ni *et al.* 2011) using Gibson cloning (Gibson *et al.* 2009; Gibson 2011). A Kozak sequence (GCCACC) was added upstream of the start codon, and the *ftz* intron between the CDS and the 3′ UTR was removed.

Single guides were cloned into pCFD3 (Port *et al.* 2014) using a *Bbs*I digest, as described in Housden *et al.* (2014). Double-guides (targeting *wg*, *hnt*, *cut*, and *elav*) were cloned into pCFD4 (Port *et al.* 2014) using Gibson cloning, following the author's protocols. All guide sequences are available in Supporting Information, Table S1. Nuclease efficiency scores were calculated using the algorithm described in Housden *et al.* (2014), accessed via an online tool (http://www.flyrnai.org/evaluateCrispr/). Briefly, these values are based on an empirical analysis of the cutting efficiency of a library of sgRNAs, based on the position of each nucleotide at each of the 20 positions within the protospacer.

Cell culture and transfection

S2R+ cells were cultured in Schneider's *Drosophila* medium (Millipore, Gibco) containing 10% fetal bovine serum and penicillin/streptomycin (at 1000 units/ml and 1000 mcg/ml, respectively). Cells were transfected using Effectene Transfection Reagent (Qiagen) using the manufacturer's protocol, except that twice the number of recommended suspension cells were seeded per well. For pActin-driven experiments, 50 ng of gRNAs and 150 ng dCas9 were transfected in 24-well plates. For UAS experiments, equal amounts (either 66 or 100 ng) of all components were transfected in 12- or 24-well plates.

Quantitative PCR

Three or four days after transfection, total RNA was collected using TRIZOL (Life Technologies) following the manufacturer's instructions. Total RNA was purified using an RNeasy MinElute Cleanup Kit (Qiagen), including a 30-min on-column DNase treatment. Equal volumes of total RNA were used as template for first-strand complementary DNA (cDNA) synthesis using the iScript cDNA synthesis kit (Bio-Rad). Quantitative PCR (qPCR) was conducted using iQ Supermix (Bio-Rad) on a C1000 Thermal Cycler (Bio-Rad), and fold-change was calculated using the $2^{\Delta\Delta Ct}$ method (Livak and Schmittgen 2001), with error propagated using standard methods and with *rp49* as a reference gene. The primers used for qPCR are listed in Table S2.

Western blotting

Cells were harvested 3 days after transfection. The following primary antibodies were used: anti-tubulin (Sigma T5168, 1:10,000), anti-Wg (4D4; DSHB, 1:400), anti-Hnt (1G9; DSHB, 1:500), anti-Cas9 (Abcam 191468, 1:500), and anti-FLAG (Sigma F3165, 1:10,000), with 5% BSA as a blocking reagent. HRP-coupled sheep anti-mouse (Amersham NXA931, 1:5000) was used as a secondary antibody, and signal was detected with Pierce ECL or SuperSignal West Pico reagents (Thermo).

RNAseq

S2R+ cells were transfected with Actin:dCas9-VPR along with either a negative control sgRNA that does not target the *Drosophila* genome (QUAS #1; Table S1) or a pool of five sgRNAs targeting either *snail*, *twist*, or a combination of both pools (Table S1). Total RNA was obtained as described above, and RNA integrity was confirmed by Bioanalyzer (Agilent). Between 2.0 and 2.5 M 100-bp single-end reads were generated for each sample using Illumina Hi-Seq at the Columbia Genome Center, following standard protocols for Illumina library preparation and sequencing. Reads were mapped to the *Drosophila melanogaster* genome (BDGP R5 assembly) using TopHat (Trapnell *et al.* 2009), and only uniquely mapped reads (between 76.4 and 83.3% of the reads for each sample) were used for further analysis. FPKM and read count values were obtained using Cufflinks (Trapnell *et al.* 2010) and HTSeq (Anders *et al.* 2015), respectively. Two biological replicates were sequenced per sample, and duplicate runs were highly correlated (Pearson's correlation ≥0.99 for all experiments). To eliminate potentially confounding effects of low read counts, we filtered out genes with <1 of 1 M reads recorded for each sample. The "nbionomTest" of the Bioconductor package DESeq (Anders

and Huber 2010) was then used to obtain differentially expressed gene lists at a multiple hypothesis testing-adjusted *P*-value of 0.05.

For each activation experiment, we defined the target genes as the union of the (1) differentially expressed genes in induced sample compared to control sample and (2) genes that are not expressed (0 or very few reads) in control but highly expressed in induced samples or vice versa. These gene lists were used for Gene Ontology (GO) analysis and further comparison with chromatin immunoprecipitation (ChIP) data.

To compare our data with published ChIP data, we downloaded Snail and Twist ChIP data from the Berkeley *Drosophila* transcription Network Project (MacArthur *et al.* 2009) (http://bdtnp.lbl.gov/Fly-Net/) and updated the wiggle file genome coordinates to the R5 genome assembly. We then pooled binding-site information of the two replicates and identified genes with the nearest TSS to the binding peak as the putative target gene. Read stacks were generated using the Integrated Genomics Visualizer (Robinson *et al.* 2011) after pooling the two BAM files for each experiment.

All RNAseq data have been deposited in Gene Expression Omnibus (accession no. GSE71430).

Transgenic flies

Transgenic 10X-UAS:3xFLAG-Cas9-VP64 and VPR constructs and double sgRNA-plasmids in pCFD4 (both described above) were integrated into the attP40 landing site on the second chromosome (Markstein *et al.* 2008) using standard phiC31 transformation methods.

For activation experiments, flies of the genotype *w;UAS:dCas9-VP64*/CyO;*dpp-Gal4/TM6b,Tb* or *w;UAS:dCas9-VPR*/CyO;*dpp-Gal4/TM6b,Tb* were crossed to homozygous sgRNA-*wg* flies (*yv;sgRNA-wg*). Wing discs from non-Tb larvae (*i.e.*, those containing *dpp*-Gal4) were costained with an anti-FLAG antibody to differentiate those larvae expressing the activator constructs from their siblings receiving the CyO balancer chromosome and an anti-Wg antibody to test for ectopic Wg expression.

Immunohistochemistry

In vivo experiments were conducted at 27°. Wandering-stage larval wing discs were dissected in PBS, fixed for 25–30 min in 4% paraformaldehyde in PBS, and then stained using standard protocols. Antibodies used were mouse anti-Wingless (4D4; DSHB, 1:100) and rabbit anti-FLAG (Sigma F7425, 1:500). Secondary antibodies coupled to Alexa 488 and 555 (Invitrogen) were used at 1:400, samples were imaged on a Zeiss LSM 780 confocal microscope, and maximum-intensity projections are shown.

Results and Discussion

Human codon-optimized dCas9-VPR works robustly in Drosophila cells

We first compared the activity of the published dCas9-VPR activator, which is human codon-optimized and contains four nuclease-attenuating mutations (D10A, H839A, H840A, and N863A), to a *Drosophila* codon-optimized dCas9-VPR that contains two of these mutations (D10A and H840A), thought to be sufficient to remove nuclease activity (Mali *et al.* 2013; Perez-Pinera *et al.* 2013) (Figure 1A). We cotransfected these constructs, under UAS control, together with a plasmid encoding pActin-Gal4, and pairs of two sgRNAs targeting a window from −400 to −50 upstream of the TSS of two endogenous genes: *wingless* (*wg*) and *hindsight* (*hnt*, aka *pebbled*). We confirmed efficient translation of all of the activator constructs via Western blot (Figure 1B), demonstrating that differential activity was not due to activator protein levels.

In all four cases, the published Hs-dCas9-VPR construct substantially outperformed dCas9-VP64 and Dm-dCas9-VPR (Figure 1, C and D). The superior performance of Hs-dCas9-VPR was seen both via qPCR (Figure 1C) and via Western blots against the target genes (Figure 1D). It is unlikely that codon optimization caused this difference, as the two VPR constructs were expressed at equivalent levels (Figure 1B), suggesting that the four nuclease-attenuating mutations may be important for maximal function. We used the Hs-dCas9-VPR construct (hereafter shortened to "dCas9-VPR") in all subsequent experiments.

To test whether dCas9-VPR can activate a range of target genes, we cotransfected cells with Actin:dCas9-VPR with pools of two to six sgRNAs targeting each of eight additional genes (*per*, *y*, *os*, *en*, *AttC*, *Dro*, *twi*, and *Sna*). In all cases, we observed robust activation ranging over two orders of magnitude (Figure 1E). Importantly, we note that two additional genes that we targeted (*cut* and *elav*) were not upregulated using either of two pairs of sgRNAs per gene (data not shown). In agreement with previous reports (Chavez *et al.* 2015; Konermann *et al.* 2015), we found that the level of activation of a given gene was inversely correlated with its basal expression level (Figure S1). In other words, dCas9 activation is most effective for genes that are expressed at low levels in a given cell type and does not strongly upregulate genes that are already transcriptionally active.

Design principles for sgRNAs

The initial characterization of dCas9-VPR employed pools of up to five sgRNAs per target gene (Chavez *et al.* 2015). We therefore wanted to know whether such groups of sgRNAs have synergistic effects or whether a single guide within the pool is largely responsible for activation. To address this question, we transfected three guides that target upstream of the TSS of a reporter construct (QUAS:Luciferase), both singly and in combination. The effect of the pooled sgRNAs could be almost completely attributed to the activity of a single highly active sgRNA with an essentially additive effect of the other two minimally active guides (Figure 2A). Next, we tested five nonoverlapping guides targeting immediately upstream of two endogenous genes, *twist* and *engrailed*. In both cases, there was marked heterogeneity in guide efficiency, with one guide giving substantially higher activation than
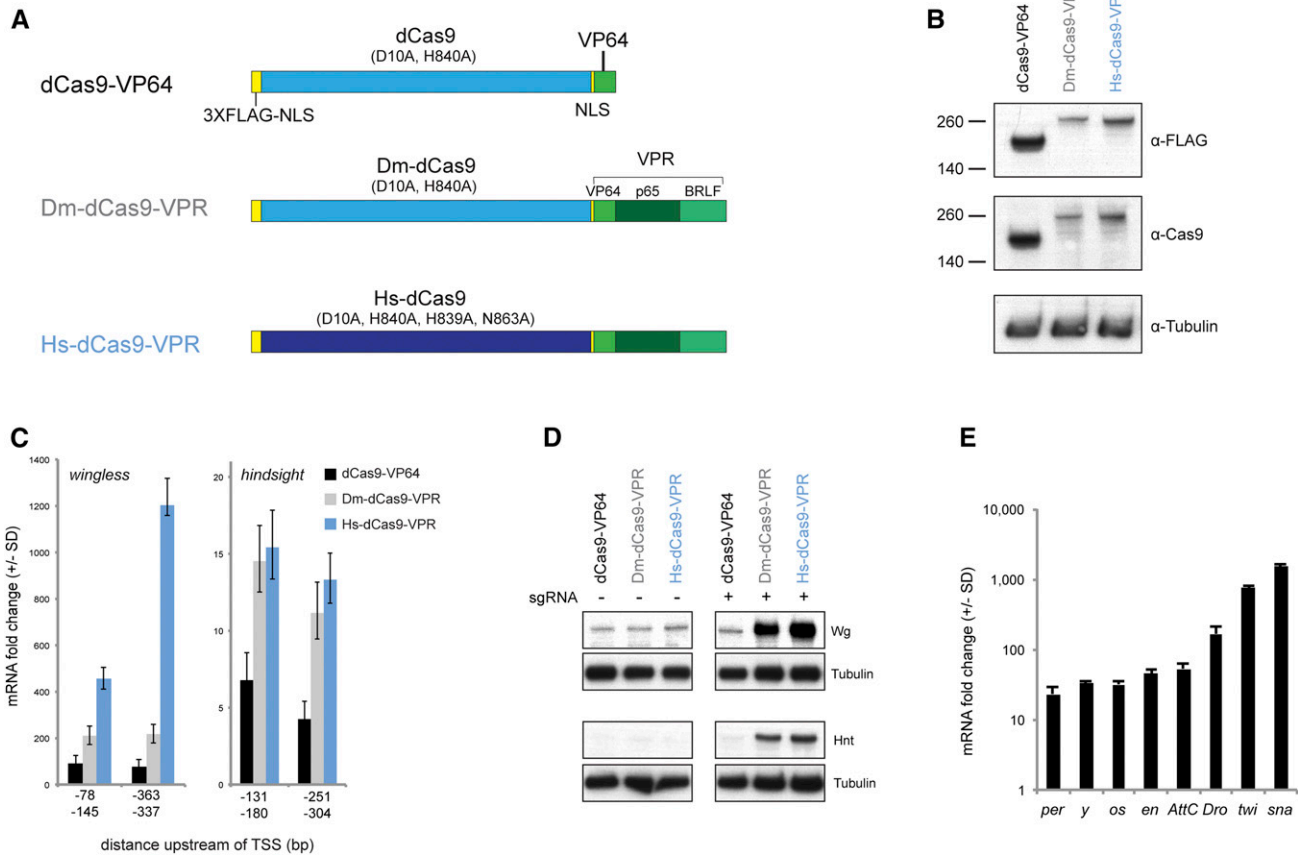
Figure 1 dCas9-VPR activates target gene expression in *Drosophila* S2R+ cells. (A) Schematics of the constructs tested in this study. Dm-dCas9 is codon-optimized for *Drosophila*, Hs-dCas9 for human. (B) Western blot analysis of dCas9 activators demonstrating that constructs are effectively translated. (C) qPCR analysis of *wg* and *hnt* activation. For each gene, two pairs of sgRNAs located upstream of the TSS were tested. Each sgRNA pair was expressed from a single plasmid driving expression from the U6:3 and U6:1 promoters, respectively (see *Materials and Methods*). (D) Western blot analysis of Wg and Hnt activation. (E) qPCR analysis of eight additional endogenous genes by Hs-dCas9-VPR. In B–D, UAS-driven constructs were cotransfected with pActin-Gal4. In E, Hs-dCas9-VPR was expressed using the Actin promoter.

any of the others (Figure 2B). Recent studies utilizing alternative Cas9-activator strategies have similarly found that individual sgRNAs vary widely in their ability to activate target gene activity (Tanenbaum *et al.* 2014; Konermann *et al.* 2015). These differences in activation are not correlated to the predicted sgRNA nuclease efficiency score, which is based on empirical analysis of cutting efficiency relative to the probability of a given nucleotide at each of the 20 positions within the sgRNA (Figure S2A) (Housden *et al.* 2014). Neither are these differences due to differential sgRNA-binding capability, as activation levels were uncorrelated with sgRNA GC content (Figure S2B). Furthermore, sgRNA performance was not related to differential bioavailability, as sgRNA concentration was not limiting over the wide range of concentrations tested (Figure S2C). Together, these results suggest that certain single sgRNAs are largely responsible for activation, but we do not currently understand the specific design principals for these particularly effective sgRNAs.

We next considered the effect of sgRNA placement relative to the TSS. Two previous studies have systematically examined the effect of sgRNA placement relative to the TSS (Gilbert

et al. 2014; Konermann *et al.* 2015). Gilbert *et al.* (2014) calculated an optimal window of activation range from −400 to −50 bp upstream of the TSS, whereas Konermann *et al.* (2015) found that a smaller window from −100 to 0 bp upstream of the TSS is optimal. In our experiments, the most active sgRNA was not necessarily within 100 bp of the TSS, and we observed that several sgRNAs within this window were not effective (Figure 2B). Furthermore, our experiments with pairs of sgRNAs targeting *wg* (Figure 1C) showed that a pair of sgRNAs located −337 and 363 bp upstream of the TSS gave far better activation than a pair at −78 and −145 bp upstream, while a trend in the opposite direction was true for *hnt*. Together, our results demonstrate that it is important to test a variety of sgRNAs in a window from −400 to 0 upstream of the TSS to maximize activation. We suggest that a good compromise for future studies is to express sgRNAs from the pCFD4 plasmid (Port *et al.* 2014), which contains sites for co-expression of two separate sgRNAs driven by the U6:3 and U6:1 promoters, respectively.

Many sgRNAs targeting early in the first exon of genes have been generated by a variety of laboratories for the purpose of
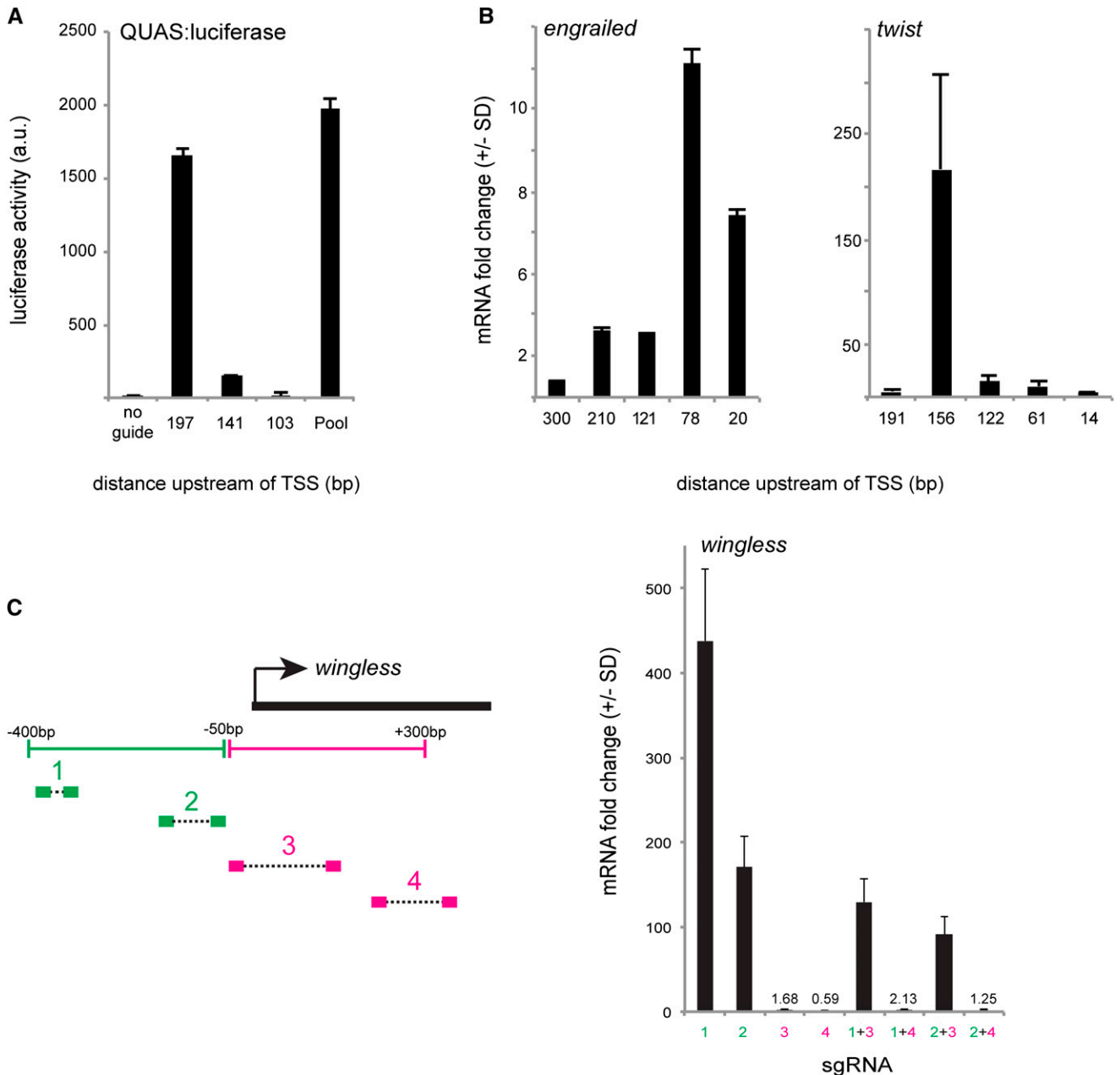
Figure 2 Effects of individual sgRNA on target gene activation. (A) Three nonoverlapping sgRNAs tiling the region upstream of a QUAS:luciferase reporter construct were transfected either singly or in combination. (B) Five nonoverlapping sgRNAs targeting the upstream region of two endogenous genes, *engrailed* and *twist*, differ in their effectiveness. (C) Four pairs of sgRNAs targeting the regions upstream and downstream of the *wg* TSS were tested singly and in combination. sgRNAs downstream of the TSS do not activate transcription, and their presence can reduce or completely block transcription in the presence of an effective sgRNA.

generating null mutations via Cas9-mediated mutagenesis (reviewed in Housden *et al.* 2014). We therefore asked whether such existing sgRNA reagents could be useful for Cas9-mediated transcriptional activation. However, previous studies have shown that dCas9–sgRNA complexes targeting in the first exon, downstream of the TSS, can prohibit activation by blocking transcript elongation (Cheng *et al.* 2013; Qi *et al.* 2013). To verify this in our system, we examined the activation efficiency of four pairs of sgRNAs targeting a region from −400 bp upstream to 400 bp downstream of the *wg* TSS, both singly

and in combination. sgRNAs targeting downstream of the TSS did not activate transcription, and in fact these sgRNAs reduced or completely blocked the effect of upstream sgRNAs (Figure 2C). In agreement with previous studies (Qi *et al.* 2013), sgRNAs targeting the minus strand had a much stronger repressive effect (Figure 2C, "3" on the plus strand and "4" on the negative strand.) We therefore conclude that Cas9-activator studies should avoid using sgRNAs that target downstream of the TSS. These guides, however, may prove useful for future studies using dCas9 for transcriptional repression.

Identification of transcription factor targets using multiplexed Cas9 activation and RNAseq

Cas9-based transcriptional activation has the notable benefit that multiple genes can be simultaneously targeted using a pool of sgRNAs (Zalatan *et al.* 2014; Chavez *et al.* 2015; Konermann *et al.* 2015). We validated the efficacy of multiplexed gene activation in *Drosophila* cells by cotransfecting Actin:dCas9-VPR with guides targeting three target genes: *twist*, *snail*, and *engrailed*. We observed robust activation of all three genes singly, as pairs, and as a pool of three (Figure S3).

Given the effectiveness of dCas9-VPR, we reasoned that combining Cas9-based activation with RNAseq should provide a conceptually simple approach for identifying transcription factor target genes. We focused on Twist and Snail, two highly conserved transcription factors that function in the *Drosophila* embryo to specify mesoderm specification and subsequent development (Leptin 1991). Twist is a basic helix-loop-helix activator (Thisse *et al.* 1988; Murre *et al.* 1989), and Snail is a zinc-finger transcription factor, classically considered to be a repressor (Boulay *et al.* 1987; Nieto 2002; Barrallo-Gimeno and Nieto 2005). However, a recent study has suggested that Snail may have additional roles as a transcriptional activator (Rembold *et al.* 2014). Importantly, the genome-wide targets of both genes have been characterized via independent means, allowing for direct comparison with our data (Sandmann *et al.* 2007; Zeitlinger *et al.* 2007; Macarthur *et al.* 2009).

We transfected S2R+ cells with sgRNAs targeting *twist* and *snail* singly and in combination (5 sgRNAs per gene), as well as a nontargeting sgRNA negative control, and then used RNAseq to identify differentially expressed genes. This approach should identify direct and indirect targets of both genes (*i.e.*, genes that are secondarily activated by direct targets) and should identify target genes of both factors individually, as well as those genes that are only activated by both factors acting together.

RNAseq confirmed that *snail* and *twist* themselves were highly activated by dCas9-VPR, whether targeted singly or together (Figure 3, A–C; Table S3). In each experiment, we also identified a number of additional genes that were significantly differentially expressed (*P*-value cutoff = 0.05) following overexpression of *twist* (66 genes), *snail* (27 genes), or both (106 genes; Figure 3, A–C; Table S3).

One important caveat is that dCas9-VPR may have off-target activation effects (Kuscu *et al.* 2014; Wu *et al.* 2014). Indeed, it has been shown that dCas9 is capable of binding to DNA sequences with up to nine consecutive mismatches in the PAM-distal region (Kuscu *et al.* 2014). We therefore analyzed each of the predicted off-target binding sites according this rule (Gratz *et al.* 2014) and asked whether any nearby gene is upregulated in our RNAseq experiments. Among 77 potential off-target sites for the *snail* or *twist* sgRNAs, 5 fell near genes that were differentially expressed in our analysis. While 3 of these genes were also near ChIP sites for Twist or Snail, and thus may be genuine targets, 2 are not near ChIP peaks (*CG32813* and *CG15154*) and should be considered off-target effects. In future studies, we strongly recommend using one of the existing online sgRNA

design tools to minimize off-target binding sites in the genome (reviewed in Housden *et al.* 2014).

Gene Ontology enrichment analysis showed that the genes coregulated by Snail and Twist are enriched for terms related to mesoderm and muscle development, as expected (Figure 3D). A subset of these terms was also significantly enriched among targets of Twist alone, including muscle organ development ($P = 0.003163$), but no terms were following Snail activation alone, consistent with the observation that these factors act synergistically (Rembold *et al.* 2014). Furthermore, of the genes upregulated by Snail and Twist together, 38 genes (35.8%) were upregulated only upon co-expression of Snail + Twist. Repression of target genes, as opposed to activation, was observed in a substantially higher proportion of Snail-regulated genes than Twist-regulated genes (37.0 compared to 7.6%), consistent with the observation that Snail commonly acts as a repressor (Barrallo-Gimeno and Nieto 2005). However, we also noted that Snail and Twist together led to the down-regulation of 23 genes not repressed by either factor individually (Table S3), suggesting that the presence of Twist may contribute to the repressive activity of Snail, although this effect could be indirect, *i.e.*, mediated by an additional factor that is regulated by Twist and/or Snail.

To begin to differentiate between direct and indirect targets, we calculated the proportion of differentially expressed genes that are adjacent to known ChIP peaks for *snail* and *twist*. A highly significant proportion of our predicted target genes were adjacent to ChIP peaks for the relevant factor ($P < 0.0001$; χ^2 test; Figure 3E), suggesting that these are direct Snail and Twist targets. These include known target genes such as *heartless* (Shishido *et al.* 1993), *inflated* (Sandmann *et al.* 2007), and *escargot* (Fuse *et al.* 1996) (Figure 3F and Table S3) and also include new, uncharacterized targets such as *CG6330* and *CG3376* (Figure 3F). For the target gene *CG3376*, Snail and Twist had opposite effects on the expression levels, but in combination led to an increase in *CG3376* levels (Figure 3F). In contrast, for the majority of target genes identified in this study, we observed that *snail* and *twist*, both singly and in combination, promoted target gene activation rather than repression, consistent with recent observations that *snail* has a dual role as a transcriptional activator (*e.g.*, *htl* and *esg*, Figure 3F). The remaining genes, which are not adjacent to ChIP peaks, are likely indirect targets (Table S3).

The number of differentially expressed genes in the present study is far less than the number of observed ChIP peaks (representing between 1.3 and 6.8% of the ChIP peaks; Figure 3E). This difference may be partially due to the difference in cell type (S2R+ cells *vs.* embryonic tissue) or false positives from ChIP experiments based on cross-linking conditions, but we suggest that this may also reflect the fact that transcription factor occupancy does not necessarily correlate with transcription. Because the approach described here relies on a direct analysis of target gene transcription, it should therefore be less prone to false positives than ChIP studies.

In vivo activation using dCas9-VPR

To date, all studies of Cas9 activators have been conducted in cell culture, and *in vivo* activation has not yet been demonstrated in
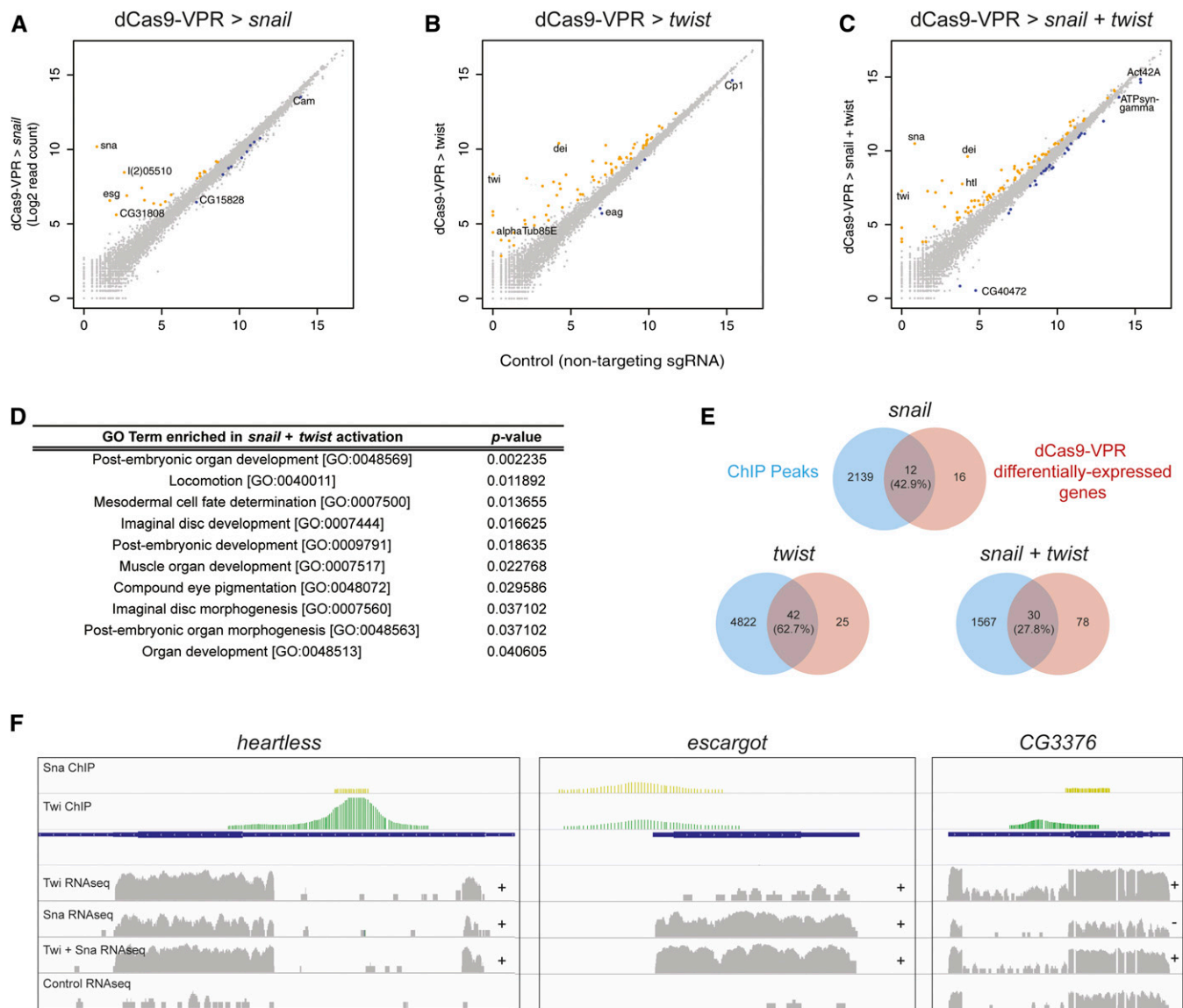
Figure 3 Identification of *snail* and *twist* target genes using dCas9-VPR and RNAseq. (A–C) Differential expression analysis following activation of *snail* (A), *twist* (B), or both (C). Read counts are plotted on a $\log_2$ scale. Colored circles indicate significant difference from control values at $P < 0.05$. (D) GO term enrichment for *snail* + *twist* targets, including several terms associated with mesoderm development. (E) Venn diagrams demonstrating the proportion of differentially expressed genes that also show ChIP peaks for *snail*, *twist*, or both. (F) Representative examples showing RNAseq data together with previous ChIP data. The "+" and "−" indicate significant upregulation and downregulation, respectively, relative to control expression levels.

any multicellular animal (Gilbert *et al.* 2014; Tanenbaum *et al.* 2014; Zalatan *et al.* 2014; Chavez *et al.* 2015; Konermann *et al.* 2015). We therefore tested whether the dCas9-VPR system functions *in vivo* in *Drosophila*.

We generated transgenic flies expressing either dCas9-VP64 or dCas9-VPR under UAS control, as well as a line that constitutively expresses two sgRNAs targeting *wg*. Expression of these transgenes was not toxic, as driving these constructs ubiquitously using Actin-Gal4 was not lethal (data not shown). As a proof of principle, we used *dpp*-Gal4 to drive expression of the dCas9-VP64 or dCas9-VPR in a stripe of expression along the anterior–posterior margin in the larval wing disc. We crossed *dpp*-Gal4 > UAS:dCas9-activator flies to sgRNA-*wg* flies and examined Wg expression using

immunostaining. In the wild type, Wg is expressed in a stripe along dorsal–ventral margin, perpendicular to the *dpp*-Gal4 expression domain (Figure 4, A and A′). Strikingly, the dCas9-VPR construct drove ectopic Wg expression (Figure 4, C and C′), while the dCas9-VP64 did not (Figure 4, B and B′), consistent with our cell culture data. To show that this ectopic Wg expression is physiologically relevant, we examined the morphology of these wing discs and observed a partial duplication of the wing pouch and other patterning abnormalities, consistent with ectopic activation using *dpp*-Gal4 > UAS:Wg (Figure 4, A″–C″) (Ng *et al.* 1996). These *dpp*-Gal4 > dCas9-VPR, sgRNA-*wg* larvae died during early pupal stages, precluding analysis of adult wing morphology. Thus, dCas9-VPR can activate physiologically
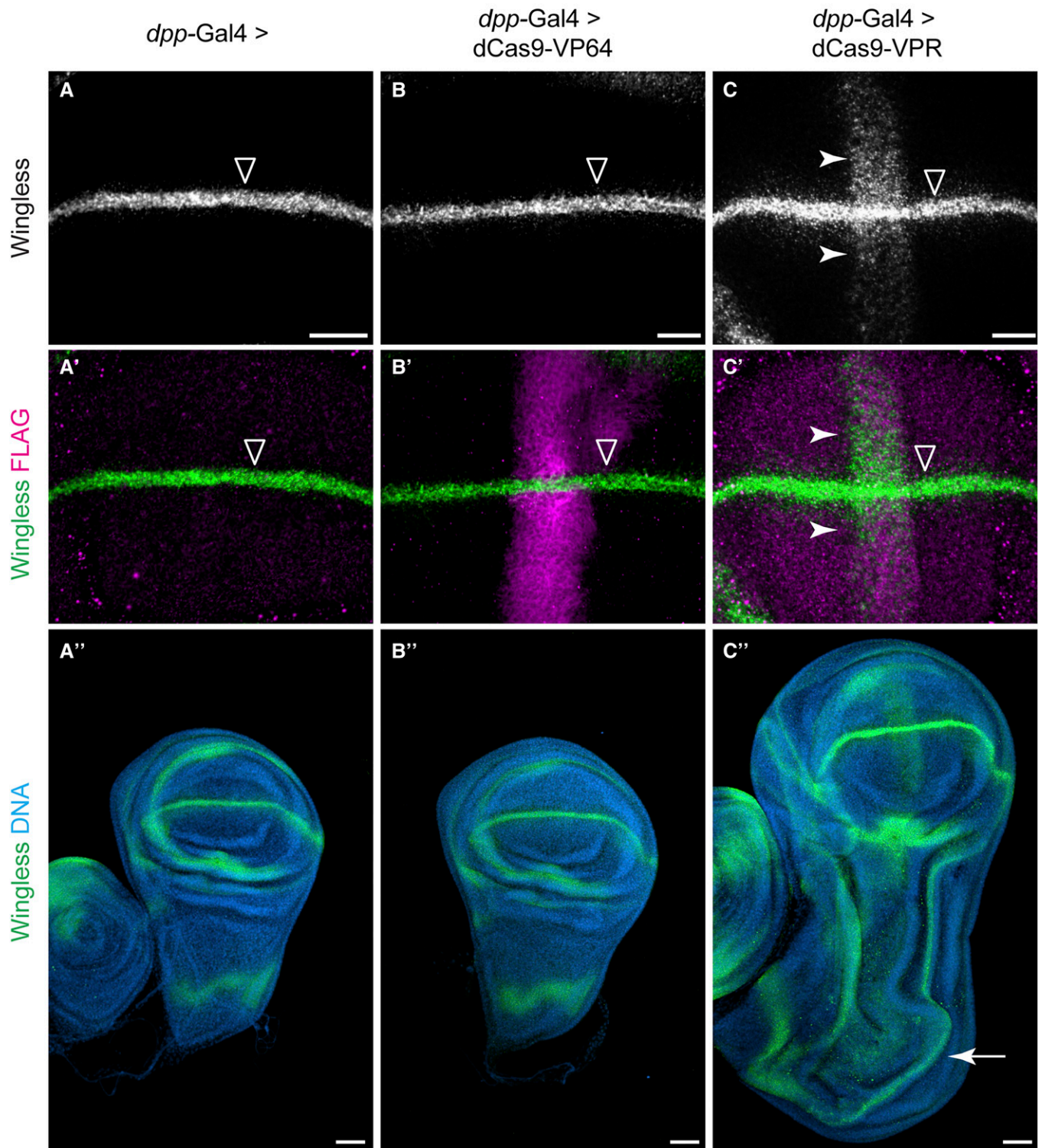
Figure 4 *In vivo* activation using dCas9-VPR. Flies homozygous for sgRNA-*wg* (two sgRNAs) were crossed to flies containing *dpp*-Gal4 driving expression of UAS-3X-FLAG:dCas9 activators. (A and A') In the absence of dCas9 activator, Wg is expressed in a stripe along the dorsal–ventral wing margin (open arrowhead). (B and B') *dpp*-Gal4 > dCas9-VP64 did not activate ectopic Wg, despite high levels of transgene expression. (C and C') *dpp*-Gal4 > dCas9-VPR activates a stripe of ectopic Wg expression (white arrowhead). The dCas9-VPR transgene is expressed at relatively low levels compared to dCas9-VP64 (compare C' to B'). (C'') Ectopic activation of Wg using dpp-Gal4 > dCas9-VPR leads to a partial duplication of the wing pouch (white arrow). See *Materials and Methods* for full genotypes. Bar: 20 μm in A–C' and 50 μm in A''–C''.

relevant levels of target gene expression and can generate dominant phenotypes *in vivo*.

Conclusion

In this study, we demonstrate the ease and effectiveness of the dCas9-VPR system for activating target genes both in *Drosophila* cells and *in vivo*. Based on our observations that a single sgRNA targeting within ∼400 bp upstream of the TSS can be used to activate target genes, but that sgRNAs differ widely in their efficiency, we propose that a good compromise is to express two sgRNAs per target gene from a single plasmid, using a vector such as pCFD4 (Port *et al.* 2014). Our results also show that sgRNAs targeting downstream of the TSS are not compatible with dCas9-based activation, consistent with previous studies (Qi *et al.* 2013). In addition, our results also support previous reports (Chavez *et al.* 2015; Konermann *et al.* 2015) that target gene activation levels are inversely proportional to that gene's basal expression level, which suggests that dCas9-based activation is most effective for genes that are expressed at low levels in a given cell type. Furthermore, we have shown that dCas9-VPR, combined with RNAseq, can be applied to identify targets of transcription factors in multiplex.

Finally, we have provided the first demonstration of Cas9-based activation *in vivo*, demonstrating that this strategy holds great potential for overexpression studies. For *in vivo* studies involving stable transgenic organisms, the dCas9-VPR strategy has the benefit that it requires only a single dCas9 component, in contrast to the other existing strategies (Gilbert *et al.* 2014; Tanenbaum *et al.* 2014; Zalatan *et al.* 2014; Chavez *et al.* 2015; Konermann *et al.* 2015). The dCas9-VPR strategy that we describe here will make it possible to produce genome-scale transgenic sgRNA lines for overexpression screens, thus complementing other approaches such as random UAS-insertion lines ("EP lines") (Rørth 1996; Staudt *et al.* 2005) and UAS-ORF lines (Bischof *et al.* 2013).

Literature Cited

Anders, S., and W. Huber, 2010   Differential expression analysis for sequence count data. Genome Biol. 11: R106.

Anders, S., P. T. Pyl, and W. Huber, 2015   HTSeq: a Python framework to work with high-throughput sequencing data. Bioinformatics 31: 166–169.

Barrallo-Gimeno, A., and M. A. Nieto, 2005   The Snail genes as inducers of cell movement and survival: implications in development and cancer. Development 132: 3151–3161.

Bischof, J., M. Bjorklund, E. Furger, C. Schertel, J. Taipale *et al.*, 2013   A versatile platform for creating a comprehensive UAS-ORFeome library in Drosophila. Development 140: 2434–2442.

Boulay, J. L., C. Dennefeld, and A. Alberga, 1987   The Drosophila developmental gene snail encodes a protein with nucleic acid binding fingers. Nature 330: 395–398.

Chavez, A., J. Scheiman, S. Vora, B. W. Pruitt, and M. Tuttle *et al.*, 2015   Highly efficient Cas9-mediated transcriptional programming. Nat. Methods 12: 326–328.

Chen, S., N. E. Sanjana, K. Zheng, O. Shalem, K. Lee *et al.*, 2015   Genome-wide CRISPR screen in a mouse model of tumor growth and metastasis. Cell 160: 1–16.

Cheng, A. W., H. Wang, H. Yang, L. Shi, Y. Katz *et al.*, 2013   Multiplexed activation of endogenous genes by CRISPR-on, an RNA-guided transcriptional activator system. Cell Res. 23: 1163–1171.

Fuse, N., S. Hirose, and S. Hayashi, 1996   Determination of wing cell fate by the escargot and snail genes in Drosophila. Development 122: 1059–1067.

Gibson, D. G., 2011   Enzymatic assembly of overlapping DNA fragments. Methods Enzymol. 498: 349–361.

Gibson, D. G., L. Young, R.-Y. Chuang, J. C. Venter, C. A. Hutchison *et al.*, 2009   Enzymatic assembly of DNA molecules up to several hundred kilobases. Nat. Methods 6: 343–345.

Gilbert, L. A., M. H. Larson, L. Morsut, Z. Liu, G. A. Brar *et al.*, 2013   CRISPR-mediated modular RNA-guided regulation of transcription in eukaryotes. Cell 154: 442–451.

Gilbert, L. A., M. A. Horlbeck, B. Adamson, J. E. Villalta, Y. Chen *et al.*, 2014   Genome-scale CRISPR-mediated control of gene repression and activation. Cell 159: 1–15.

Gratz, S. J., F. P. Ukken, C. D. Rubinstein, G. Thiede, L. K. Donohue *et al.*, 2014   Highly specific and efficient CRISPR/Cas9-catalyzed homology-directed repair in *Drosophila*. Genetics 196: 961–971.

Housden, B. E., S. Lin, and N. Perrimon, 2014   Cas9-based genome editing in Drosophila. Methods Enzymol. 546: 415–439.

Housden, B. E., A. J. Valvezan, C. Kelley, R. Sopko, S. Lin *et al.*, 2015   Identification of potential drug targets for Tuberous Sclerosis Complex by synthetic screens combining CRISPR-based knockouts with RNAi. Science Signaling (in press).

Konermann, S., M. D. Brigham, A. E. Trevino, J. Joung, O. O. Abudayyeh *et al.*, 2015   Genome-scale transcriptional activation by an engineered CRISPR-Cas9 complex. Nature 517: 583–588.

Kuscu, C., S. Arslan, R. Singh, J. Thorpe, and M. Adli, 2014   Genome-wide analysis reveals characteristics of off-target sites bound by the Cas9 endonuclease. Nat. Biotechnol. 32: 1–9.

Leptin, M., 1991   twist and snail as positive and negative regulators during Drosophila mesoderm development. Genes Dev. 5: 1568–1576.

Livak, K. J., and T. D. Schmittgen, 2001   Analysis of relative gene expression data using real-time quantitative PCR and the $2-\Delta\Delta CT$ method. Methods 25: 402–408.

MacArthur, S., X.-Y. Li, J. Li, J. B. Brown, H. C. Chu *et al.*, 2009   Developmental roles of 21 Drosophila transcription factors are determined by quantitative differences in binding to an overlapping set of thousands of genomic regions. Genome Biol. 10: R80.

Maeder, M. L., S. J. Linder, V. M. Cascio, Y. Fu, Q. H. Ho *et al.*, 2013   CRISPR RNA-guided activation of endogenous human genes. Nat. Methods 10: 977–979.

Mali, P., J. Aach, P. B. Stranges, K. M. Esvelt, M. Moosburner *et al.*, 2013 CAS9 transcriptional activators for target specificity screening and paired nickases for cooperative genome engineering. Nat. Biotechnol. 31: 833–838.

Markstein, M., C. Pitsouli, C. Villalta, S. E. Celniker, and N. Perrimon, 2008 Exploiting position effects and the gypsy retrovirus insulator to engineer precisely expressed transgenes. Nat. Genet. 40: 476–483.

Murre, C., P. S. McCaw, and D. Baltimore, 1989 A new DNA binding and dimerization motif in immunoglobulin enhancer binding, daughterless, MyoD, and myc proteins. Cell 56: 777–783.

Ng, M., F. J. Diaz-Benjumea, J. P. Vincent, J. Wu, and S. M. Cohen, 1996 Specification of the wing by localized expression of wingless protein. Nature 381: 316–318.

Ni, J.-Q., R. Zhou, B. Czech, L.-P. Liu, L. Holderbaum *et al.*, 2011 A genome-scale shRNA resource for transgenic RNAi in Drosophila. Nat. Methods 8: 405–407.

Nieto, M. A., 2002 The snail superfamily of zinc-finger transcription factors. Nat. Rev. Mol. Cell Biol. 3: 155–166.

Perez-Pinera, P., D. D. Kocak, C. M. Vockley, A. F. Adler, A. M. Kabadi *et al.*, 2013 RNA-guided gene activation by CRISPR-Cas9-based transcription factors. Nat. Methods 10: 973–976.

Port, F., H.-M. Chen, T. Lee, and S. L. Bullock, 2014 Optimized CRISPR/Cas tools for efficient germline and somatic genome engineering in Drosophila. Proc. Natl. Acad. Sci. USA 111: E2967–E2976.

Qi, L. S., M. H. Larson, L. A. Gilbert, J. A. Doudna, J. S. Weissman *et al.*, 2013 Repurposing CRISPR as an RNA-guided platform for sequence-specific control of gene expression. Cell 152: 1173–1183.

Rembold, M., L. Ciglar, J. O. Yanez-Cuna, R. P. Zinzen, C. Girardot *et al.*, 2014 A conserved role for Snail as a potentiator of active transcription. Genes Dev. 28: 167–181.

Robinson, J. T., H. Thorvaldsdóttir, W. Winckler, M. Guttman, E. S. Lander *et al.*, 2011 Integrative genomics viewer. Nat. Biotechnol. 29: 24–26.

Rørth, P., 1996 A modular misexpression screen in Drosophila detecting tissue-specific phenotypes. Proc. Natl. Acad. Sci. USA 93: 12418–12422.

Sandmann, T., C. Girardot, M. Brehme, W. Tongprasit, V. Stolc *et al.*, 2007 A core transcriptional network for early mesoderm development in Drosophila melanogaster. Genes Dev. 21: 436–449.

Shishido, E., S. Higashijima, Y. Emori, and K. Saigo, 1993 Two FGF-receptor homologues of Drosophila: one is expressed in mesodermal primordium in early embryos. Development 117: 751–761.

Staudt, N., A. Molitor, K. Somogyi, J. Mata, S. Curado *et al.*, 2005 Gain-of-function screen for genes that affect Drosophila muscle pattern formation. PLoS Genet. 1: e55.

Tanenbaum, M. E., L. A. Gilbert, L. S. Qi, J. S. Weissman, and R. D. Vale, 2014 A protein-tagging system for signal amplification in gene expression and fluorescence imaging. Cell 159: 635–646.

Thisse, B., C. Stoetzel, C. Gorostiza-Thisse, and F. Perrin-Schmitt, 1988 Sequence of the twist gene and nuclear localization of its protein in endomesodermal cells of early Drosophila embryos. EMBO J. 7: 2175–2183.

Trapnell, C., L. Pachter, and S. L. Salzberg, 2009 TopHat: discovering splice junctions with RNA-Seq. Bioinformatics 25: 1105–1111.

Trapnell, C., B. A. Williams, G. Pertea, A. Mortazavi, G. Kwan *et al.*, 2010 Transcript assembly and quantification by RNA-Seq reveals unannotated transcripts and isoform switching during cell differentiation. Nat. Biotechnol. 28: 511–515.

Wu, X., D. A. Scott, A. J. Kriz, A. C. Chiu, P. D. Hsu *et al.*, 2014 Genome-wide binding of the CRISPR endonuclease Cas9 in mammalian cells. Nat. Biotechnol. 32: 1–9.

Zalatan, J. G., M. E. Lee, R. Almeida, L. A. Gilbert, E. H. Whitehead *et al.*, 2014 Engineering complex synthetic transcriptional programs with CRISPR RNA scaffolds. Cell 160: 1–12.

Zeitlinger, J., R. P. Zinzen, A. Stark, M. Kellis, H. Zhang *et al.*, 2007 Whole-genome ChIP-chip analysis of Dorsal, Twist, and Snail suggests integration of diverse patterning processes in the Drosophila embryo. Genes Dev. 21: 385–390.

Communicating editor: J. Sekelsky

GENETICS

In Vivo Transcriptional Activation Using CRISPR/Cas9 in *Drosophila*

Shuailiang Lin, Ben Ewen-Campen, Xiaochun Ni, Benjamin E. Housden, and Norbert Perrimon
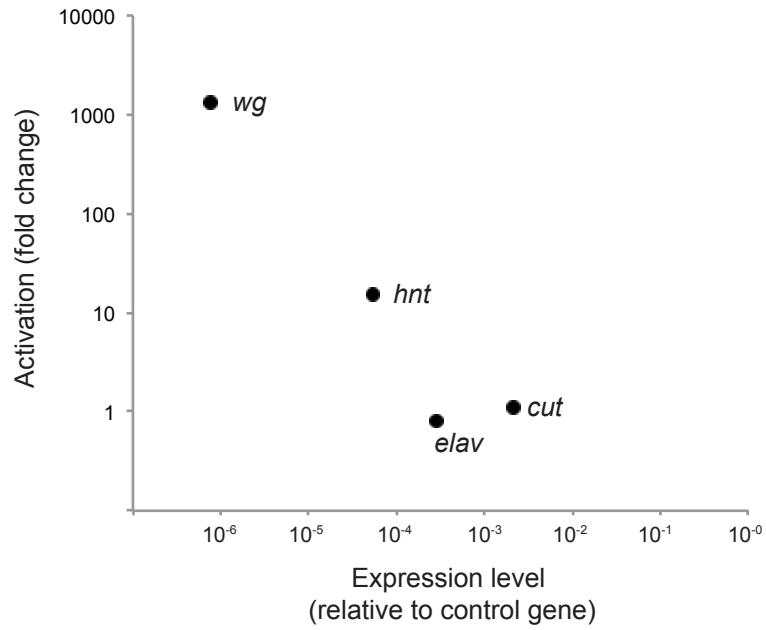
Figure S1. Cas9 activation of target genes is inversely proportional to basal expression levels. The activation level (fold change) is plotted against the relative expression level for four genes tested in parallel. Relative expression levels are estimated based on the difference in Ct values between the basal expression level of the target gene and a control gene, *Rp49*.
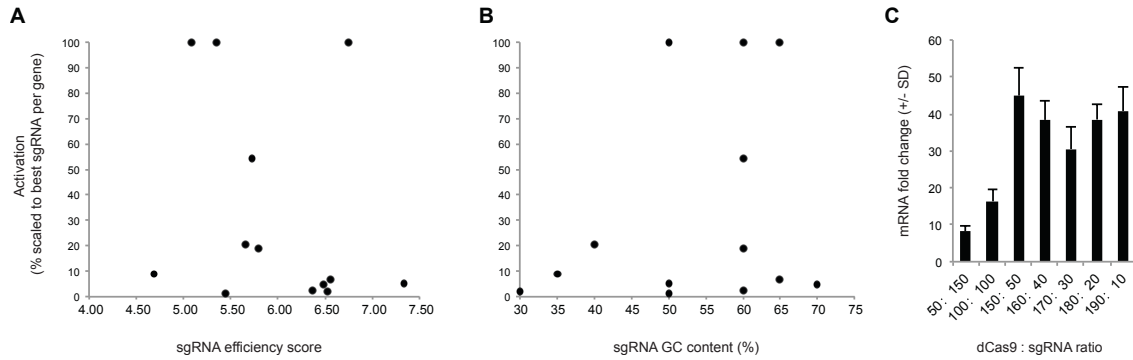
Figure S2. sgRNA effectiveness is not related to nuclease efficiency or GC content, and sgRNAs are not rate limiting in these experiments. (A) 13 sgRNAs targeting 3 genes (QUAS:luciferase, *twist*, and *engrailed*) are shown plotted against the predicted nuclease efficiency score. The activation for each sgRNA is shown as a percentage of the best-performing sgRNA for that gene. There is no correlation between sgRNA activation and efficiency score. (B) The same sgRNAs as in (A) are shown plotted against sgRNA GC content, revealing no correlation. (C) dCas9-VPR activation is robust over a wide range of dCas9 : sgRNA ratios, indicating that sgRNA availability is not limiting in our experiments.
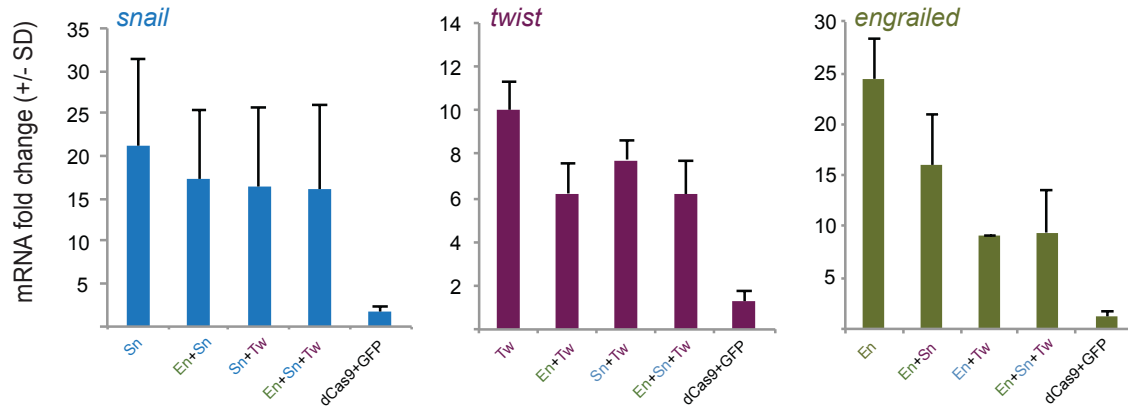
Figure S3. Simultaneous activation of multiple target genes using multiplexed guides. Three endogenous genes (*sna, twi,* and *en*) were robustly activated when activated using pairs of sgRNAs or a pool of three sgRNAs.

Table S1   sgRNAs used in this study. Distances from TSS are based on BDGP
Release 6 (August 2014).

Gene targeted	sgRNA sequence (including PAM)	Distance from TSS (from 3' end of PAM)	Strand	Efficiency Score
wg	CCCCGATCCGATCGCATCGTCGG	-78	minus	4.85
	GCAGCTGCAATGCAGGAGTCAGG	-145	plus	4.07
wg	ATGAGGTTGCGCAAATAATCGGG	-363	plus	6.79
	GGAAATGGAAAAACTCTGCCCGG	-337	minus	4.26
wg	TATATATTGTATCGTAAATTTGG	125	minus	5.33
	ATTTGTGCGATTAATTCCGCTGG	206	minus	5.79
wg	GCTGCTGACAAACGCAGAGTCGG	22	plus	5.39
	CGTGTGTTTCAGTTAAGCGTTGG	15	plus	7.97
hnt	GCGCAAATAGGATTACACATTGG	-251	minus	4.63
	GGGCCGTACTCATCTTTCATTGG	-304	minus	3.41
hnt	GAGAGAAGAGAGAAGCAGTCTGG	-131	minus	4.55
	ATTTGAAACGAAGAATGAGAAGG	-180	plus	5.30
hnt	AGTTGTATTTATAAATACAACGG	34	minus	4.86
	TGCGTTTGATATTTCTTTGTAGG	173	minus	6.56
hnt	GCCTAAAACAGTGCGAAATCCGG	444	plus	4.81
	AACAGTGCGAAATCCGGAGTTGG	450	plus	5.66
QUAS (#1)	CTCGGGTAATCGCTTATCCTCGG	-103	plus	5.45
QUAS (#2)	CGGATAAACAATTATCCTCACGG	-141	plus	4.69
QUAS (#3)	CCAACGCGTTGGGAGCTCTCCGG	-197	plus	5.35
engrailed (isoform A)	GCGTTAACTCTCCCCGACGTCGG	-20	plus	5.72

engrailed (isoform A)	AACTGTCACGGTGGAAAGAGAGG	-78	minus	5.09
engrailed (isoform A)	GGCGAGATCCCACAAGTAGCTGG	-121	minus	5.80
engrailed (isoform A)	AGCGAAAATCGATCAGTGTAAGG	-210	plus	5.65
engrailed (isoform A)	GCTCACTCACTCCTATTAGCTGG	-300	minus	7.33
twist (isoform B)	CAAAATGTCAATTTGAGCAATGG	-14	plus	6.52
twist (isoform B)	GCGGGACGACGATAGAGCGGCGG	-61	plus	6.48
twist (isoform B)	GCCATCCCGCTCCCACTCAATGG	-122	minus	6.56
twist (isoform B)	GCATCGGCAGGTATGACGTCAGG	-156	minus	6.75
twist (isoform B)	ATTTTCTCGAGCGGCAGCGGCGG	-191	minus	6.37
per	GAGTGAGTGTGAGAAAATTCTGG	-50	minus	5.85
per	CCGCCGTCGCTGAGAATCGCTGG	-104	plus	6.38
per	TCGCTCGGGAAATCGCTGGTCGG	-136	plus	6.03
per	TTCGCCCAAGGGTTAATGTTTGG	-151	minus	6.05
y	CATTGGCCTGTCTTCGTCTTCGG	-46	minus	6.83
y	ACGAAGGCGCGCGCCAACTTCGG	-101	plus	7.86
y	ATTCGGGTGGTTCAGTGTTCGGG	-135	plus	6.55
y	CGCAAAGTTGGCCGATCTATGGG	-157	minus	4.45
Os	TACCGCTCGTCGGCACTCGGCGG	-39	minus	4.91
Os	ATTCAGATCCGAAGAACCGCAGG	-131	plus	6.27
en	GCGTTAACTCTCCCCGACGTCGG	-19	minus	5.72
en	AACTGTCACGGTGGAAAGAGAGG	-77	plus	5.09
en	GGCGAGATCCCACAAGTAGCTGG	-120	plus	5.80
en	AGTGAGTGAGTGACAGCAGTTGG	-164	plus	4.10
en	AGCGAAAATCGATCAGTGTAAGG	-209	minus	5.65
en	GCTCACTCACTCCTATTAGCTGG	-299	plus	7.33

AttC	TATAGCAATCTATCTCTGAGTGG	-48	plus	6.52
AttC	TATAAATTGGTATTCATTGTCGG	-63	minus	6.64
AttC	AGCTGAGCAATGTTTCGCACTGG	-138	plus	5.61
AttC	GTGAACCACCTGGTCATTCGGGG	-140	minus	9.39
AttC	ATCCCCTTGAAACTACTTGCCGG	-209	plus	6.92
AttC	TAAAATTTGAACTTACTCATTGG	-338	minus	6.22
Dro	CGAATCTCTTGTTGCATCGATGG	-39	minus	4.31
Dro	AACATGAAAAGTCCCCAAGATGG	-101	minus	3.56
Dro	GCCGGTGATTCCCCATCTTGGGG	-112	plus	4.30
Dro	ATCAACGAATAGGCGACTGAAGG	-151	plus	5.78
Dro	GCTGCGTAGTTTACATCATTCGG	-220	plus	5.30
sna	CCGACGCCGCTGTCGCCATTTGG	-68	plus	7.39
sna	TCCATTTCCCACCTCTCTCTCGG	-235	plus	8.15
sna	AAAGTGCTGTTGTTGTTGCTAGG	-117	minus	7.14
sna	GAAATACGCAATAAGGGTATGGG	-141	minus	5.39
sna	GAGAGAGAGAGTGAGAGAGCAGG	-179	minus	5.96

Table S2   qPCR primers used in this study.

Gene targeted	Forward Primer	Reverse Primer
Rp49	ATCGGTTACGGATCGAACAA	GACAATCTCCTTGCGCTTCT
wingless	CCAAGTCGAGGGCAAACAGAA	TGGATCGCTGGGTCCATGTA
hindsight	ACATCCGGTGCCACAATTA	AGGGATGAAGCCGAGGATAGC
snail	CGGAACCGAAACGTGACTAT	CCTTTCCGGTGTTTTTGAAA
twist	AAGTCCCTGCAGCAGATCAT	CGGCACAGGAAGTCAATGTA
engrailed	TCCGTGATCGGTGACATGAGT	CGCCGACGTATCATCCACATC
period	GACTCGGCCTACTCGAACAG	CGCGACTTATCCTTGTTGCG
yellow	TACCTGTTGGAGTCGAACACT	GTGGCCGGAATCCCATCAC
Os aka *upd1*	GTCGGATAAAGTAGCTAACTTGAA	AAACTTCAAGTTAGCTACTTTATC
Attacin-C	CGCCACCCAGAATCTACAGG	CTTAGGTCCAATCGGGCATCG
Drosocin	GTCGGCAACAAGAGATTCGAATGGG	AAACCCCATTCGAATCTCTTGTTGC

S. Lin et al.

Table S3 Differentially expressed genes following activation of *snail, twist*, and *snail + twist* (*p*-value cutoff = 0.05).

dCas9-activated TF	Differentially Expressed Gene	Flybase ID	CG number	Fold Change (Log2)	ChiP Peak
snail	sna	FBgn0003448	CG3956	10.06567708	Yes
snail	l(2)05510	FBgn0028622	CG13432	6.019522795	
snail	esg	FBgn0001981	CG3758	5.438088815	Yes
snail	pyr	FBgn0033649	CG13194	4.320828812	Yes
snail	Idgf4	FBgn0026415	CG1780	3.772949815	
snail	CG31808	FBgn0062978	CG31808	3.481828608	
snail	htl	FBgn0010389	CG7223	2.706344789	Yes
snail	Ggamma30A	FBgn0267252	CG3694	1.88490427	
snail	if	FBgn0001250	CG9623	1.361821658	
snail	CG31516	FBgn0051516	CG31516	1.332014094	Yes
snail	Ama	FBgn0000071	CG2198	1.282418899	Yes
snail	CG13928	FBgn0035246	CG13928	0.945532592	Yes
snail	tok	FBgn0004885	CG6863	0.785310731	Yes
snail	dally	FBgn0263930	CG4974	0.761523509	Yes
snail	CG3624	FBgn0034724	CG3624	0.710650399	
snail	CG5455	FBgn0039430	CG5455	0.701973435	
snail	hoe1	FBgn0041150	CG12787	0.683715599	
snail	CG5895	FBgn0036560	CG5895	0.535425178	
snail	CG3800	FBgn0034802	CG3800	-0.419648113	
snail	CG12099	FBgn0035232	CG12099	-0.428194298	
snail	CG5118	FBgn0031317	CG5118	-0.463998841	
snail	CG3860	FBgn0034951	CG3860	-0.562885083	Yes
snail	tmod	FBgn0082582	CG1539	-0.58824945	Yes
snail	Cap-H2	FBgn0037831	CG14685	-0.629304699	
snail	CG33926	FBgn0053926	CG33926	-0.634353699	
snail	CG8547	FBgn0033919	CG8547	-0.640350549	
snail	Paip2	FBgn0038100	CG12358	-0.722847538	
snail	CG3376	FBgn0034997	CG3376	-0.801759241	Yes
twist	CG15611	FBgn0034194	CG15611	Inf	
twist	CG15658	FBgn0034602	CG15658	Inf	Yes
twist	CG17270	FBgn0038828	CG17270	Inf	
twist	acj6	FBgn0000028	CG9151	Inf	
twist	alphaTub85E	FBgn0003886	CG9476	Inf	
twist	ect	FBgn0000451	CG6611	Inf	
twist	twi	FBgn0003900	CG2956	Inf	Yes
twist	lmd	FBgn0039039	CG4677	Inf	Yes
twist	dei	FBgn0263118	CG5441	6.248589419	Yes
twist	PGRP-LB	FBgn0037906	CG14704	6.13543379	
twist	CCKLR-17D3	FBgn0030954	CG32540	4.434007846	Yes
twist	htl	FBgn0010389	CG7223	3.936688181	Yes

S. Lin et al.

twist	nvy	FBgn0005636	CG3385	3.64454539	Yes
twist	e	FBgn0000527	CG3331	3.638143579	
twist	alpha-Est1	FBgn0015568	CG1031	3.505377756	Yes
twist	btn	FBgn0014949	CG5264	3.409022052	Yes
twist	CG3376	FBgn0034997	CG3376	3.017699542	Yes
twist	CG13707	FBgn0035578	CG13707	2.995481719	Yes
twist	CG6231	FBgn0038720	CG6231	2.984047614	Yes
twist	Pu	FBgn0003162	CG9441	2.887683306	
twist	CG17032	FBgn0036547	CG17032	2.829535333	
twist	sano	FBgn0034408	CG12758	2.805911606	Yes
twist	CG9150	FBgn0031775	CG9150	2.792648879	
twist	Bili	FBgn0039282	CG11848	2.424495665	Yes
twist	CG12402	FBgn0038202	CG12402	2.287528386	Yes
twist	pyd3	FBgn0037513	CG3027	1.849919318	Yes
twist	trol	FBgn0267911	CG33950	1.813775804	Yes
twist	kon	FBgn0032683	CG10275	1.792138095	Yes
twist	Fuca	FBgn0036169	CG6128	1.759441705	
twist	SerT	FBgn0010414	CG4545	1.68233002	
twist	CG17181	FBgn0035144	CG17181	1.441725877	Yes
twist	CG7149	FBgn0031948	CG7149	1.440411931	
twist	if	FBgn0001250	CG9623	1.396773256	Yes
twist	CG18557	FBgn0031470	CG18557	1.328767553	
twist	Mmp1	FBgn0035049	CG4859	1.236089352	
twist	CG13506	FBgn0034723	CG13506	1.229569672	Yes
twist	rut	FBgn0003301	CG9533	1.228660489	Yes
twist	CG30089	FBgn0050089	CG30089	1.152076771	Yes
twist	nkd	FBgn0002945	CG11614	1.150717399	Yes
twist	CG6406	FBgn0034269	CG6406	1.067665782	
twist	RhoL	FBgn0014380	CG9366	1.04021967	Yes
twist	CG14741	FBgn0037989	CG14741	0.997668804	
twist	CG32813	FBgn0052813	CG32813	0.994802235	
twist	CG8451	FBgn0031998	CG8451	0.963138737	
twist	zormin	FBgn0052311	CG33484	0.903534883	Yes
twist	CG5916	FBgn0038401	CG5916	0.898968909	
twist	CG10962	FBgn0030073	CG10962	0.880539393	
twist	CG33116	FBgn0053116	CG33116	0.864437342	Yes
twist	Sans	FBgn0033785	CG13320	0.853707309	
twist	sick	FBgn0263873	CG43720	0.786380378	Yes
twist	CG42806	FBgn0261975	CG42806	0.743647143	
twist	ash2	FBgn0000139	CG6677	0.713986802	Yes
twist	CG7872	FBgn0030658	CG7872	0.680440718	Yes
twist	Pax	FBgn0041789	CG31794	0.660397209	Yes
twist	CG4802	FBgn0034215	CG4802	0.57850087	
twist	miple2	FBgn0029002	CG18321	0.560957173	Yes
twist	SP1173	FBgn0035710	CG10121	0.558605324	Yes
twist	argos	FBgn0062279	CG4531	0.552945125	Yes
twist	CG6522	FBgn0034223	CG6522	0.544987319	
twist	Fit2	FBgn0036688	CG7729	0.50990303	Yes

twist	Rac2	FBgn0014011	CG8556	0.442453783	Yes
twist	CG32772	FBgn0052772	CG32772	0.437854963	Yes
twist	lig3	FBgn0038035	CG17227	-0.451475123	Yes
twist	dnr1	FBgn0260866	CG12489	-0.498567259	Yes
twist	Cp1	FBgn0013770	CG6692	-0.753112048	Yes
twist	CG6206	FBgn0027611	CG6206	-0.885978932	Yes
twist	eag	FBgn0000535	CG10952	-1.207357152	Yes
snail + twist	CG42741	FBgn0261705	CG42741	Inf	
snail + twist	acj6	FBgn0000028	CG9151	Inf	
snail + twist	ect	FBgn0000451	CG6611	Inf	
snail + twist	twi	FBgn0003900	CG2956	Inf	Yes
snail + twist	CG17270	FBgn0038828	CG17270	Inf	
snail + twist	sna	FBgn0003448	CG3956	10.37275099	Yes
snail + twist	esg	FBgn0001981	CG3758	6.140652322	Yes
snail + twist	l(2)05510	FBgn0028622	CG13432	5.543924262	
snail + twist	dei	FBgn0263118	CG5441	5.457144722	
snail + twist	PGRP-LB	FBgn0037906	CG14704	5.243935125	
snail + twist	CCKLR-17D3	FBgn0030954	CG32540	4.025529417	
snail + twist	htl	FBgn0010389	CG7223	3.884987587	Yes
snail + twist	pyr	FBgn0033649	CG13194	3.618856076	Yes
snail + twist	CG17032	FBgn0036547	CG17032	2.718094087	
snail + twist	kon	FBgn0032683	CG10275	2.374588248	
snail + twist	sano	FBgn0034408	CG12758	2.307298725	Yes
snail + twist	Ggamma30A	FBgn0267252	CG3694	2.120862762	
snail + twist	CG9150	FBgn0031775	CG9150	2.001881127	
snail + twist	nvy	FBgn0005636	CG3385	2.00178281	Yes
snail + twist	CG9896	FBgn0034808	CG9896	1.904522714	
snail + twist	Pu	FBgn0003162	CG9441	1.838598354	
snail + twist	Idgf4	FBgn0026415	CG1780	1.806214988	
snail + twist	CG4793	FBgn0028514	CG4793	1.76408991	
snail + twist	CG8834	FBgn0033733	CG8834	1.705449418	
snail + twist	trol	FBgn0267911	CG33950	1.703599489	
snail + twist	CG31516	FBgn0051516	CG31516	1.655366594	Yes
snail + twist	CG4301	FBgn0030747	CG4301	1.552425865	
snail + twist	CG3376	FBgn0034997	CG3376	1.544037935	Yes
snail + twist	btn	FBgn0014949	CG5264	1.491184766	
snail + twist	SerT	FBgn0010414	CG4545	1.482499914	
snail + twist	v	FBgn0003965	CG2155	1.410454787	Yes
snail + twist	if	FBgn0001250	CG9623	1.408778131	
snail + twist	CG17321	FBgn0032719	CG17321	1.246291866	
snail + twist	CG6639	FBgn0032638	CG6639	1.213727183	
snail + twist	CG13928	FBgn0035246	CG13928	1.199289325	Yes
snail + twist	Aph-4	FBgn0016123	CG1462	1.185869675	
snail + twist	CG32813	FBgn0052813	CG32813	1.170251895	
snail + twist	SKIP	FBgn0051163	CG31163	1.169680202	Yes
snail + twist	Pka-C3	FBgn0000489	CG6117	1.127181861	Yes
snail + twist	Ama	FBgn0000071	CG2198	1.125932052	Yes

snail + twist	CG6330	FBgn0039464	CG6330	1.112434146	
snail + twist	nemy	FBgn0261673	CG8776	1.107010595	
snail + twist	CG3624	FBgn0034724	CG3624	1.105505605	
snail + twist	CG10962	FBgn0030073	CG10962	1.036090559	
snail + twist	CG2528	FBgn0032969	CG2528	1.025803311	
snail + twist	CG7149	FBgn0031948	CG7149	1.022627635	
snail + twist	fra	FBgn0011592	CG8581	1.01197296	Yes
snail + twist	mGluRA	FBgn0019985	CG11144	1	Yes
snail + twist	CG18557	FBgn0031470	CG18557	0.992334684	
snail + twist	tok	FBgn0004885	CG6863	0.977649328	Yes
snail + twist	CG17181	FBgn0035144	CG17181	0.90838252	Yes
snail + twist	CG15097	FBgn0034396	CG15097	0.883776856	
snail + twist	skpB	FBgn0026176	CG8881	0.857066758	
snail + twist	SP1173	FBgn0035710	CG10121	0.832775786	
snail + twist	CG3655	FBgn0040397	CG3655	0.791475081	Yes
snail + twist	dally	FBgn0263930	CG4974	0.76164443	Yes
snail + twist	CG10063	FBgn0035727	CG10063	0.74594449	
snail + twist	pirk	FBgn0034647	CG15678	0.72244173	
snail + twist	Mmp1	FBgn0035049	CG4859	0.683808515	
snail + twist	CG30089	FBgn0050089	CG30089	0.663719984	Yes
snail + twist	Tret1-2	FBgn0033644	CG8234	0.633645809	
snail + twist	CG6406	FBgn0034269	CG6406	0.629092946	
snail + twist	Nrg	FBgn0264975	CG1634	0.621009959	
snail + twist	MtnA	FBgn0002868	CG9470	0.603007772	
snail + twist	CG6424	FBgn0028494	CG6424	0.547328703	Yes
snail + twist	fan	FBgn0028379	CG7919	0.540930068	
snail + twist	CG33116	FBgn0053116	CG33116	0.538053255	
snail + twist	Socs36E	FBgn0041184	CG15154	0.529432354	
snail + twist	CG42806	FBgn0261975	CG42806	0.518779062	
snail + twist	Thor	FBgn0261560	CG8846	0.510243144	Yes
snail + twist	CG10383	FBgn0032699	CG10383	0.499216614	
snail + twist	cv-c	FBgn0086901	CG34389	0.462986411	Yes
snail + twist	Lk6	FBgn0017581	CG17342	0.455326652	
snail + twist	vri	FBgn0016076	CG14029	0.450187221	Yes
snail + twist	CG6199	FBgn0036147	CG6199	0.444258864	
snail + twist	Pax	FBgn0041789	CG31794	0.434728698	Yes
snail + twist	Treh	FBgn0003748	CG9364	0.43307025	
snail + twist	Rcd5	FBgn0263832	CG1135	0.412392851	
snail + twist	Hsc70-3	FBgn0001218	CG4147	0.364419757	
snail + twist	Cct1	FBgn0041342	CG1049	0.352345712	Yes
snail + twist	CG8801	FBgn0028473	CG8801	0.346977902	
snail + twist	CG12030	FBgn0035147	CG12030	-0.337722248	
snail + twist	CG42668	FBgn0261550	CG42668	-0.371017471	
snail + twist	SelD	FBgn0261270	CG8553	-0.388574036	
snail + twist	CG32425	FBgn0052425	CG32425	-0.41109005	
snail + twist	CG10859	FBgn0032520	CG10859	-0.448912683	
snail + twist	Hexo2	FBgn0041629	CG1787	-0.451942388	
snail + twist	CG11655	FBgn0030638	CG11655	-0.484949774	Yes

S. Lin et al.

snail + twist	Act42A	FBgn0000043	CG12051	-0.487886336	
snail + twist	bys	FBgn0010292	CG1430	-0.489682006	
snail + twist	Lac	FBgn0010238	CG12369	-0.499941833	Yes
snail + twist	CG11255	FBgn0036337	CG11255	-0.50131699	
snail + twist	CG8547	FBgn0033919	CG8547	-0.56360757	
snail + twist	CG31075	FBgn0051075	CG31075	-0.566316576	
snail + twist	Mec2	FBgn0030993	CG7635	-0.597205703	
snail + twist	CG6126	FBgn0038407	CG6126	-0.602223793	
snail + twist	CG14629	FBgn0040398	CG14629	-0.631561894	
snail + twist	CG14523	FBgn0039612	CG14523	-0.639535295	
snail + twist	CG33926	FBgn0053926	CG33926	-0.645770184	
snail + twist	Cp1	FBgn0013770	CG6692	-0.726536661	
snail + twist	aru	FBgn0029095	CG4276	-0.85067735	Yes
snail + twist	CG6805	FBgn0034179	CG6805	-0.859840601	
snail + twist	CG3091	FBgn0029608	CG3091	-0.935473524	
snail + twist	BM-40-SPARC	FBgn0026562	CG6378	-0.954289606	
snail + twist	Ugt35a	FBgn0026315	CG6644	-0.954880883	
snail + twist	CG6206	FBgn0027611	CG6206	-1.137715698	
snail + twist	CG16758	FBgn0035348	CG16758	-Inf	
snail + twist	CG40472	FBgn0085736	CG40472	-Inf	

S. Lin et al.